Photodiagnosis and Photodynamic Therapy 42 (2023) 103544

Contents lists available at ScienceDirect

Photodiagnosis and Photodynamic Therapy

journal homepage: www.elsevier.com/locate/pdpdt

Label-free surface-enhanced Raman spectroscopy of serum with machine-learning algorithms for gallbladder cancer diagnosis

Wubulitalifu Dawuti [a,b,1], Jingrui Dou [a,b,1], Jintian Li [a,b], Rui Zhang [a,b], Jing Zhou [a,c], Maierhaba Maimaitiaili [a,c], Run Zhou [a,c], Renyong Lin [a,*], Guodong Lü [a,*]

[a] State Key Laboratory of Pathogenesis, Prevention, and Treatment of Central Asian High Incidence Diseases, Clinical Medical Research Institute, The First Affiliated Hospital of Xinjiang Medical University, Urumqi 830054, China
[b] School of Public Health, Xinjiang Medical University, Urumqi 830054, China
[c] College of Pharmacy, Xinjiang Medical University, Urumqi 830054, China

ARTICLE INFO

Keywords:
Gallbladder cancer (GBC)
Serum
Surface-enhanced Raman spectroscopy (SERS)
Principal component analysis-linear discriminant analysis (PCA-LDA)
Support vector machine (SVM)

ABSTRACT

Gallbladder cancer (GBC) is a rare but frequently fatal biliary tract malignancy that is typically discovered when it is already advanced. In this study, we investigated a novel technique for the quick and non-invasive diagnosis of GBC based on serum surface-enhanced Raman spectroscopy (SERS). SERS spectra of serum from 41 patients with GBC and 72 normal subjects were recorded. Principal component analysis-linear discriminant analysis (PCA-LDA), and PCA-support vector machine (PCA-SVM), Linear SVM and Gaussian radial basis function-SVM (RBF-SVM) algorithms were used to establish the classification models, respectively. When the Linear SVM was used, the overall diagnostic accuracy for classifying the two groups could achieve 97.1%, and when RBF-SVM was used, the diagnostic sensitivity of GBC was 100%. The results demonstrated that SERS combination with a machine learning algorithm is a promising candidate to be one of the diagnostic tools for GBC in the future.

1. Introduction

Gallbladder cancer (GBC) is a form of hepatobiliary malignancy that develops from the mucosal lining of the gallbladder [1]. Most patients are identified in the intermediate to late stages of the disease since the early stages of GBC are typically asymptomatic and have a high tendency for metastatic spread [2]. Therefore, the estimated 5-year overall survival of patients with GBC is less than 20% [3]. GBC pathogenesis is influenced by a number of factors, including environmental, microbial, metabolic, and molecular factors [4]. GBC has a remarkable global distribution with significant regional diversity [5]. According to the International Agency for Research on Cancer (IARC) Globocan 2018 database, 220,000 new cases of gallbladder cancer are identified each year, and the incidence rate for GBC is 12.3/100,000 for men and 27.3/100,000 for women. Gallbladder cancer accounts for 1.7% of all cancer fatalities [6,7].

GBC is distinguished by its early absence of symptoms, which makes identification and therapy difficulties [8]. At present, the clinical diagnosis of GBC mainly relies on imaging methods and serodiagnosis. The GBC is diagnosed using imaging techniques such as magnetic resonance imaging, computed tomography, contrast-enhanced ultrasonography, and ultrasonography. However, all of these techniques have limitations, which fail to detect early neoplastic changes [9]. Serological diagnosis plays an auxiliary role in imaging methods. Currently, tumor markers such as Carbohydrate Antigen 19-9 (CA 19-9) are used clinically. CA19-9 is also highly expressed in many cancers such as pancreatic cancer and cholangiocarcinoma, so it cannot be used as a specific diagnostic marker for GBC [10]. Therefore, in view of the insufficiency of the existing early diagnosis techniques, it is important that new, more sensitive, and diagnostic methods developments.

It is generally known that surface-enhanced Raman spectroscopy (SERS) has the potential to analyze biological samples and pathogens for diagnostic purposes [11]. SERS has gotten a lot of interest recently in the quest for quick, non-invasive, and accurate cancer diagnosis. SERS can detect cancer-related changes in the molecular "fingerprints" of biological liquids such as saliva, blood, and urine etc. [12]. However, because of the intricacy of the intracellular components and chemical structures, the SERS spectra from bio-samples carry a large amount of information.

* Corresponding authors.
E-mail addresses: renyonglin@xjmu.edu.cn (R. Lin), lgd_xj@qq.com (G. Lü).
[1] Contribution equally.

https://doi.org/10.1016/j.pdpdt.2023.103544
Received 20 January 2023; Received in revised form 24 March 2023; Accepted 28 March 2023
Available online 31 March 2023
1572-1000/© 2023 Elsevier B.V. All rights reserved.

The implementation of SERS in clinical practice is constrained since the extraction of rich information from big SERS data necessitates in-depth analysis by knowledgeable professionals [13].

Several areas of clinical medicine and bioengineering are now looking into machine learning. Machine learning algorithms can quickly and effectively transform large volumes of biological data into meaningful feature information [14]. The combination of SERS and machine learning is expected to become a general medical diagnostic technology [15]. The combination of machine learning and SERS can be used for rapid analysis and diagnosis for breast cancer [16], colorectal cancer [17], esophageal cancer [18], etc. However, there hasn't been any information published about the research of SERS combined with machine learning methods for GBC diagnosis.

SERS combined machine learning methods were employed in this investigation to distinguish GBC serum from serum from normal subject. We use different machine learning algorithms to build classification diagnosis models. We find that Linear SVM algorithm has better classification effect compared with other algorithms.

2. Materials and methods

2.1. Collection of serum samples

The First Affiliated Hospital of Xinjiang Medical University provided serum samples, comprising 41 from GBC patients and 72 from healthy individuals, all of which satisfied the clinical diagnostic criteria. The First Affiliated Hospital of Xinjiang Medical University's Ethical Committees granted permission to collect samples for study (Ethics No. K202107–16). According to the standard operating protocols of clinical laboratories, blood samples were drawn. The serum was then separated from the blood samples by centrifuging them at 3000 rpm for 15 min. At the end, the serum samples were frozen (−80 °C) until the SERS measurement time.

2.2. Serum SERS spectra acquisition

Using a Raman micro-spectrometer (ATR6500–785, Optosky, China) outfitted with a 785-nm laser, SERS spectra of serum samples were tested. Prior to the SERS measurement, the serum samples were thawed at room temperature. and then a mixture of 5 μl of serum and 5 μl of Ag colloid was made in a ratio of 1:1, from this mixture, 10 μl of sample was placed on an aluminum slide, and SERS spectra were captured after an air-drying period of time at room temperature. Ag colloid was purchased from Nanjing Jianzhi Instrument Equipment Co., Ltd (The silver nanoparticles were elliptical in shape with an average size of 65 × 45 nm). The wavelength calibration was done before to each online capture, and the laser power and integration time were 5 mW and 3 s. The spectral data were taken using a 20X objective lens, and the spectral range was 600–1800 cm^{-1}. Each sample is tested for 5 times, and the average value is finally taken as the spectral data of a sample. A total of 113 serum SERS spectra, comprising 41 spectra from GBC and 72 spectra from normal subjects were collected.

2.3. Spectral data pre-processing

All standard SERS data were processed using Matlab R2020a software. The important steps that require preprocessing of data in Matlab comprises of base line correction, vector normalization, and smoothing. The adaptive iteratively reweighted penalized least squares technique was used for the baseline correction [19]. processed each spectra using vector normalization [20]. All spectra were smoothed using the Savitzky-Golay smoothing process (order 5,9 points window) [21].

2.4. Data analysis using machine learning methods

The Matlab programming language (version Matlab R2020a) was used to conduct the machine learning methodologies analysis. PCA represents an unsupervised machine learning algorithm, which can decrease the dimensions of data by extracting orthogonal principal components (PCs) that interpret the maximum differences in the data. LDA and SVM, which are examples of supervised machine learning techniques, are presented for further diagnosis. These algorithms may create models that exactly predict the GBC groupings by training the algorithm using the training data. For the SVM algorithm, linear, and Gaussian radial basis function (RBF) were used to build classification models. A 7:3 ratio was used to split the entire collection of spectral data into training and testing sets [22]. The classification model was trained using the training set, and its effectiveness was assessed using the testing set. According to the findings, performance metrics were computed for the classification models, including their sensitivity, specificity, and accuracy, which can show how well they work at classifying samples [23].

3. Results and discussion

3.1. SERS spectra of the GBC and normal serum

In this investigation, the Ag colloid served as an improved substrate. In order to show the Ag colloid's enhancing effect, we acquired the SERS and Raman spectra from the same GBC serum. SERS signals were clearly visible when comparing Figs. 1(a) and (b), indicating that our Ag colloid significantly improved the serum's Raman spectra. The Ag colloid can therefore be employed as an improved substrate.

SERS spectroscopy can reveal the metabolic profiles of biological substances in different species, infer physiological changes in the body, and hence detect diseases [24]. In this work, we collected data sets from the SRES spectra of 41 GBC patients and 72 healthy people. Fig. 2(a) shows the average vector normalized SERS and standard deviation. To describe the SERS's fluctuation range, the standard deviation was employed to denote the shadow zone. Fig. 2(b) shows the difference vector normalized spectra of the GBC and normal serum SERS. According to the figure, the differences in spectral signals between normal serum and GBC were mostly concentrated at peak values of 637, 722, 810, 888, 951, 1067, 1134, 1203, 1263, 1364, 1432, and 1652 cm^{-1}. The serum SERS peak average intensity histogram with corresponding standard deviations was shown in Fig. 2(c). By using a *t*-test analysis of variance with a *p*-value (i.e., probability) cutoff of 0.05, the substantially

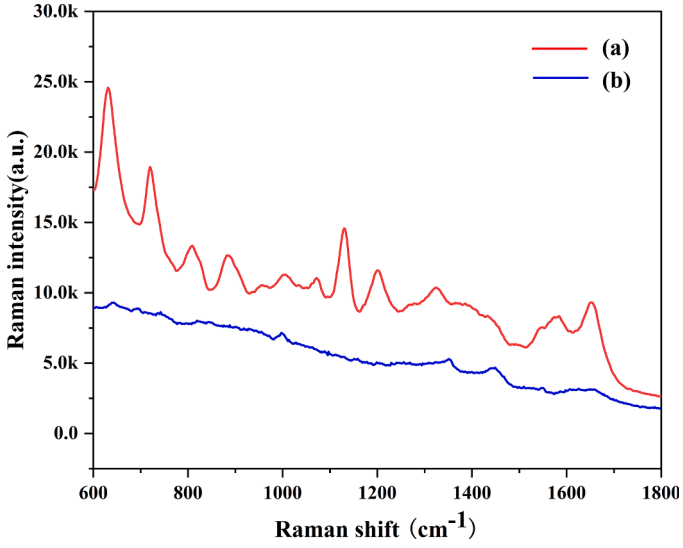


Fig. 1. (a)SERS spectra of the serum sample from a patient with GBC obtained by mixing the serum with Ag colloid at a 1:1 proportion. (b)The regular Raman spectra of serum sample from the same patient without the Ag colloid.

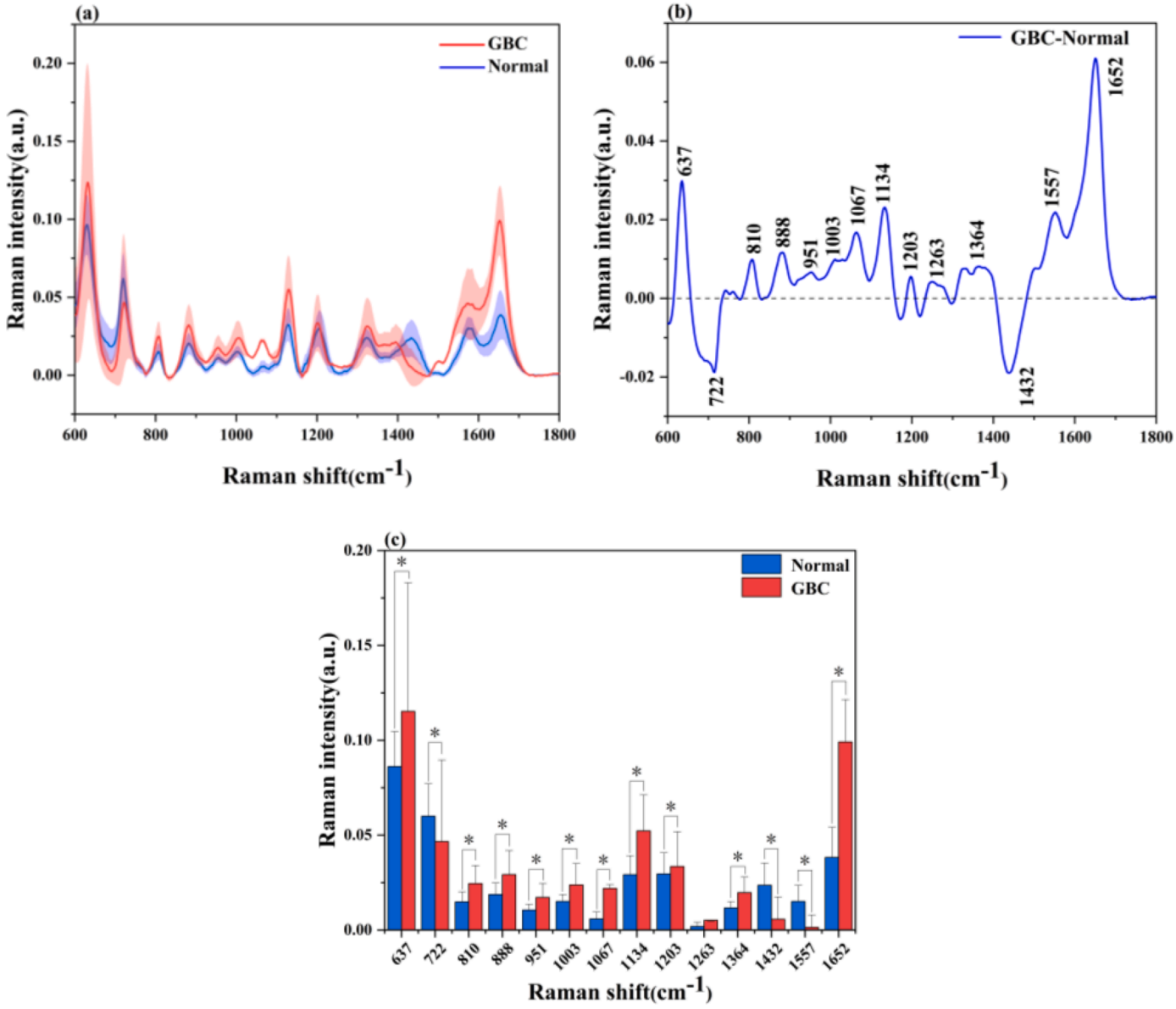


Fig. 2. (a) The average SERS of the GBC serum ($n = 41$) and normal serum ($n = 72$). The standard deviation of the mean spectral line is represented by the shaded region. (b) The difference vector normalized spectra were obtained by subtracting the average SERS of the normal serum from the average SERS of the GBC patients' serum. (c) The corresponding histograms of the average intensities and standard deviations of SERS peaks among the two groups. *p <0.05.

different peaks between the two groups were found. These differences demonstrated that progression of the GBC led to component alterations in serum biomolecules. Table 1 shows detailed data related to the peaks to aid in a better analysis. Protein, DNA, lipids, and other substances in the normal serum and the GBC serum may have somewhat different amounts. The SERS enhancement of the GBC serum was primarily concentrated in the peaks at 637 cm^{-1} (ν(C–S)), 810 cm^{-1} (ν(C–C–O)), 888 cm^{-1} (δ(C–O–H) or ring bending), 951 cm^{-1} (Single bond-stretching vibrations),1003 cm^{-1} (C—C skeletal), 1067 cm^{-1} (s (C—C)), 1134 cm^{-1} (ν(C–N)), 1203 cm^{-1} (ring vibrations), 1263 cm^{-1} (CH_2 reversing),1364 cm^{-1} (C = O stretching), 1557 cm^{-1} (NO_2 antisymmetric stretching), and 1652 cm^{-1} (C = C stretching). normal serum's high SERS intensity was mostly focused at the 722 cm^{-1} (ν(C–H)), and 1432 cm^{-1} (=CH_2 deformation). Prior SERS spectroscopic investigations on cancer found similar findings [18,25–31]. The GBC serum displayed strong SERS peaks at 810 cm^{-1} (L-serine and glutathione), 888 cm^{-1} (Tryptophan, glutathione), 1003 cm^{-1} (Phenylalanine), 1203 cm^{-1} (Phenylalanine), 1263 cm^{-1} (Amide III), 1364 cm^{-1} (Amino acid, tryptophan), 1557 cm^{-1} (Tryptophan), and 1652 cm^{-1} (Lipids), which were optical biomarkers linked to increased protein and lipid content. The SERS bands assigned to glutathione and tryptophan (810, 888, 1557, and 1364 cm^{-1}) in GBC were higher than those of the control serum samples, indicating that their presence may also be important in GBC [32]. The SERS spectrum peaks of 637 cm^{-1}(L-tyrosine, lactose) and 1134 cm^{-1}(D-mannose) were significantly higher in the GBC group's serum than in the normal group, indicating that the abnormal Glycometabolism occurs in GBC serum. The similar pattern has been observed in studies on various cancers, including colorectal cancer [31], nasopharyngeal carcinoma [33], and prostate cancer [30]. In conclusion, utilizing the different spectra, we preliminary investigated the variations between the GBC and normal serum.

To test the capability of serum SERS spectra for differentiating GBC from normal, PCA was first used to analyze SERS data. In multivariate data analysis, PCA was commonly used to reduce the number of dimensions while preserving as much variability in the data as feasible [34]. Through the production of 2D and 3D PC score graph (Fig. 3), it

Table 1
Tentative assignments of main peaks observed in SERS spectra of serum samples according to the literature [18,25–31].

Raman shift (cm^{-1})	Vibrational mode	Major assignments
637	ν(C–S)	L-tyrosine, lactose
722	ν(C–H)	Coenzyme A
810	ν(C–C–O)	L-serine, glutathione
888	δ(C–O–H) or ring bending	Tryptophan, glutathione
951	Single bond-stretching vibrations	Amino acids
1003	C-C skeletal	Phenylalanine
1067	s(C-C)	Lipids
1134	ν(C–N)	D-mannose
1203	Ring vibrations	L-tryptophan, phenylalanine
1263	CH_2 reversing	Amide III ν(C-N) of proteins
1364	C = O stretching	Amino acid, tryptophan
1432	=CH_2 deformation	N-Acetyl-Dglucosamine
1557	NO_2 antisymmetric stretching	Tryptophan
1652	C = C stretching	Lipids

was found that PC1 had a poor discrimination effect on the two groups, as PC1 only contributed 40.5% of the total variance. After adding PC2, the total contributed variance reached 72.3%, and the discrimination effect improved slightly. In addition, after adding PC3, the discrimination effect did not increase, and there is overlap between GB and healthy group samples. Therefore, further model building based on machine learning algorithms on the basis of PCA. The quantification results in the boxplots demonstrate substantial variations between the two sets of blood sample groups in each of the three SERS spaces ($P<0.001$) (Figs. 4a,c, and e). In Figs. 4b,d, and f, the loadings PC plot of two sets of samples was displayed, the PC2 successfully caught the variations/similarities present in the primary peaks, which were 637, 810, 888, 1134, and 1652 cm^{-1}. A foundation for disease-related molecular fingerprints is provided by variations in the distinctive peaks of SERS spectra.

We first extracted information variables from the SERS spectra using PCA, and then we used SVM and LDA models to further analyze how well the machine learning algorithms classified the SERS spectral data. For the SVM algorithm, linear, and Gaussian radial basis function (RBF) were used to build classification models. The performance of the models was evaluated in terms of sensitivity, specificity, and accuracy. We randomly divided the spectra data into a 70% training set and a 30% test set in order to train and evaluate the classification model [22]. A total of 113 SERS spectral data of PCA feature extraction were selected, the data of 30 GBC, and 49 normal subjects were used as to establish training model, the data of 11 GBC, and 23 normal subjects were used as the test sets to verify the diagnostic model's accuracy. Fig. 5 shows the line plot of the classification accuracy based on the PCA-LDA algorithm as the number of selected PCs increases. The black line represents the accuracy of the training set model, and the red line represents the accuracy of the validation set model. It can be seen from the figure that with the increase of the number of PCs, the accuracy of the PCA-LDA classification model gradually increases. When the number of PCs reaches 10, the accuracy of the classification model on the training set and the test set data reaches the highest value and remains stable thereafter. And the first 10 PCs explained 98.5% of the total variance. Therefore, in order to avoid the phenomenon of overfitting of the classification model, the first 10 PCs were selected as the input data for the LDA and SVM classifiers when building the model. The diagnostic sensitivity, specificity, and accuracy of PCA-SVM, PCA-LDA, Linear SVM and RBF-SVM algorithm classification models for the training set and test set were shown in Table 2 and Table 3, respectively. Figs. 6(a) and (b) were shown the 3D graphs of the diagnostic accuracy of the training set and the test set using RBF kernel SVM algorithm as a function of parameters c and g, respectively. In the training data, the sensitivity, specificity, and accuracy of RBF-SVM model for GBC and normal group were 100%. In the test model, the diagnostic sensitivity of RBF-SVM model was 100%, and the diagnostic specificity of linear SVM model was 100%. The result demonstrates that high sensitivity and specificity GBC identification may be accomplished using serum SERS spectra in combined with machine learning methods. Vu, et al. reported the study on distinguishing GBC by detection of bile juice [35]. In this study, serum was used as the detection sample, compared with bile juice, serum samples were non-invasive and easy to obtain. The SERS analysis process may be done rapidly, with a little sample volume and a simple procedure, and it has a high sensitivity and accuracy level compared to traditional clinical diagnosis methods [36]. In addition, the academia reported that SERS combined with machine learning algorithm is expected to become a universal medical diagnosis technology [15]. Therefore, we speculate that SERS spectroscopy analysis of serum with advanced machine-learning models have prospective

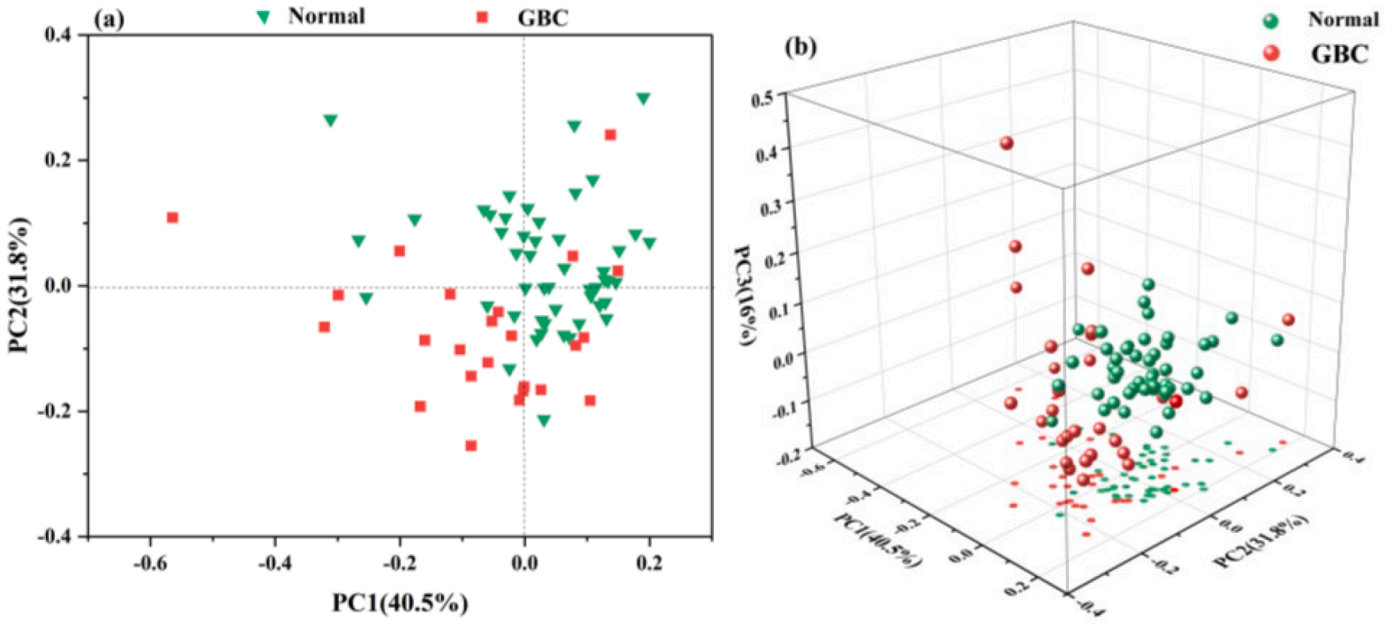


Fig. 3. (a) Two-dimensional score graph based on the PCA of the GBC and normal serum. (b) Three-dimensional score graph of the PCA corresponding to (a).

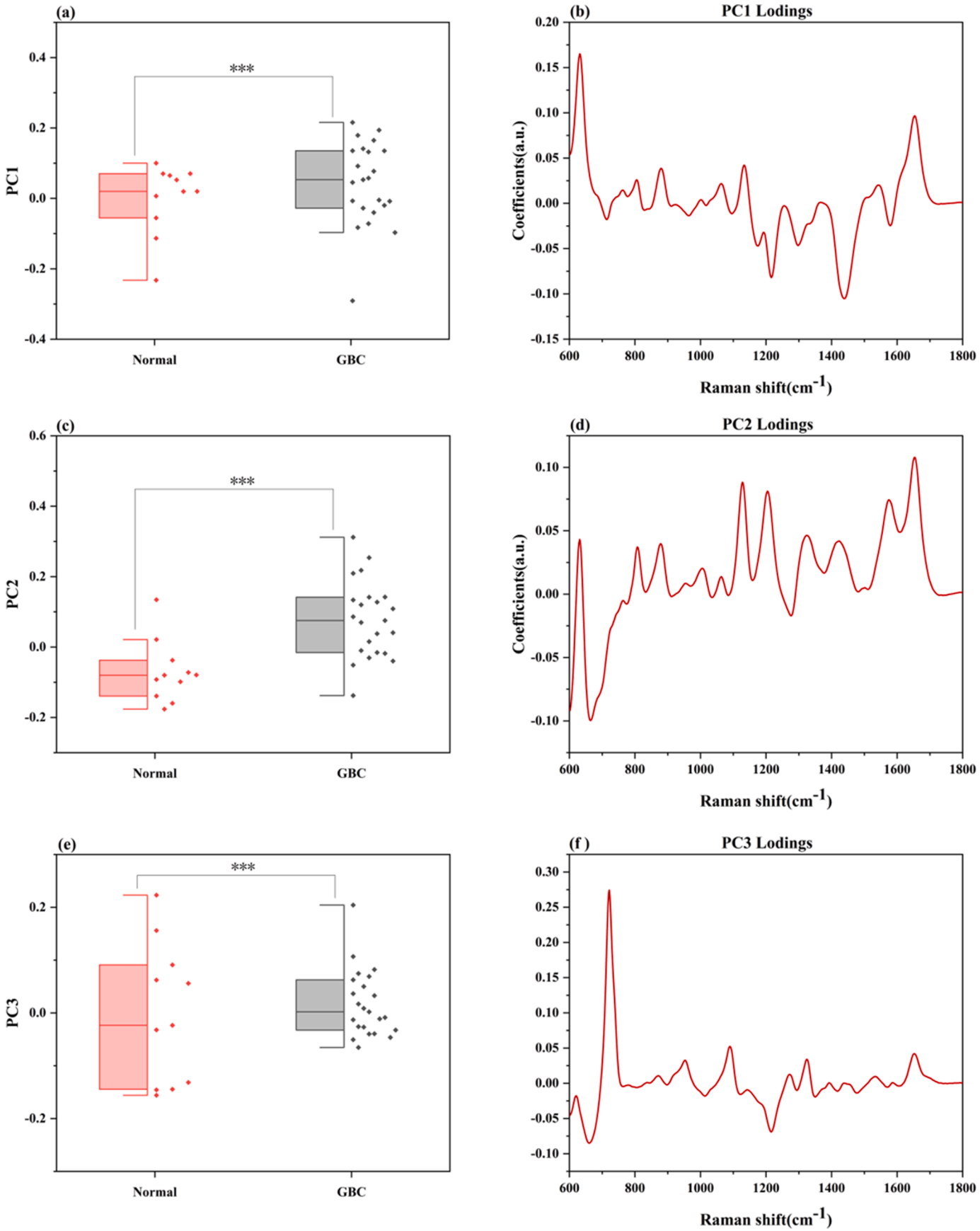


Fig. 4. Boxplots of SERS band integration of GBC and normal serum samples, showing significant differences between the two groups. (a) PC1, (c) PC2, and (e) PC3; PC means were compared by the Welch 2-sample *t*-test for unequal variances: ***$P < 0.001$. SERS loading plots of the contributions for (b) PC1, (d) PC2, and (f) PC3 are presented.

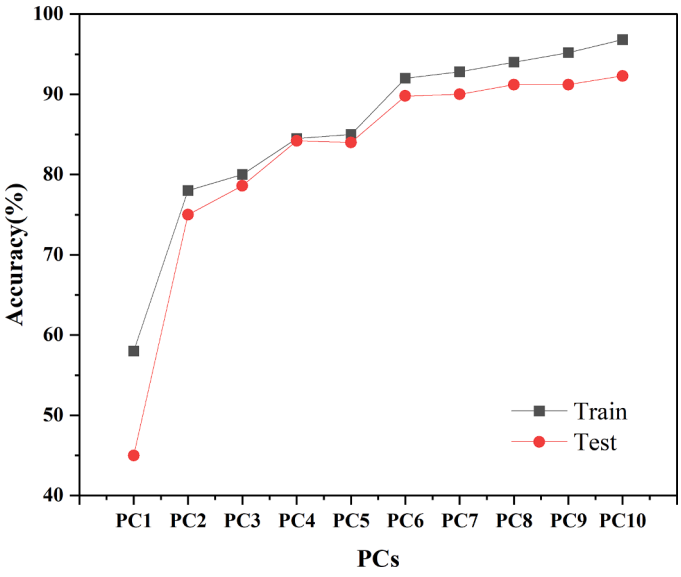


Fig. 5. Line plot of the classification accuracy of the two classifiers as the number of selected PCs increased.

application in diagnosis of GBC. The next stage in our process will be to carry out more thorough prospective studies to confirm the validity of this novel cancer detection technique.

4. Conclusion

In this study, we used silver colloid to measure the serum SERS spectra of GBC patients and normal volunteers. There is a great deal of promise to label-free diagnosis GBC utilizing serum SERS spectra using a peripheral blood sample, given the obvious discrepancies between normal and GBC serum SERS spectra. PCA-SVM, PCA-LDA, Linear SVM and RBF-SVM methods were applied to diagnose and distinguish between the GBC and normal serum, and RBF-SVM algorithm has best diagnosis effect. Overall, the findings of this exploratory investigation showed great potential for the creation of a clinical tool for the non-invasive detection and screening of GBC using SERS serum analysis.

Funding

Key research and development projects of Xinjiang Uygur Autonomous Region (2022B03013-2); Special Funds for Development of Local Science and Technology from Central Government (No. ZYYD2022B06); The projects of State Key Laboratory of Pathogenesis, Prevention and Treatment of High Incidence Diseases in Central Asian (No. SKL-HIDCA-

Table 2
Confusion matrix to distinguish between GBC and normal with different algorithms on train set.

Group	PCA-LDA		PCA-SVM		Linear SVM		RBF-SVM	
	GBC	Healthy	GBC	Healthy	GBC	Healthy	GBC	Healthy
GBC	29	1	27	3	29	1	30	0
Normal	2	47	1	48	1	48	0	49
Sensitivity (%)	96.7		90.0		96.7		100	
Specificity (%)	95.9		97.9		97.9		100	
Accuracy (%)	96.2		94.9		97.5		100	

Table 3
Confusion matrix to distinguish between GBC and normal with different algorithms on test set.

Group	PCA-LDA		PCA-SVM		Linear SVM		RBF-SVM	
	GBC	Healthy	GBC	Healthy	GBC	Healthy	GBC	Healthy
GBC	9	2	10	1	10	1	11	0
Normal	1	22	3	20	0	23	2	21
Sensitivity (%)	81.8		90.9		90.9		100	
Specificity (%)	95.7		87.5		100		91.3	
Accuracy (%)	91.2		88.2		97.1		94.1	

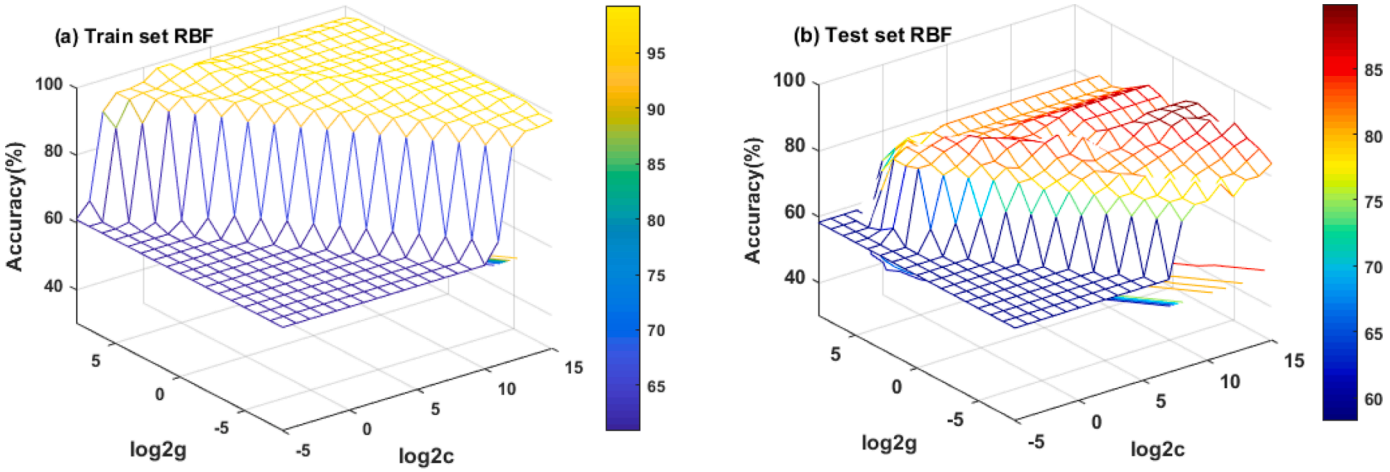


Fig. 6. (a) and (b) are 3D graphs of the diagnostic accuracy of the training set and the test set using RBF kernel SVM algorithm as a function of parameters c and g, respectively.

2021-YG1 and SKL-HIDCA-2020-BC3); The Xinjiang Tianshan Talent program (No. 2022TSYCCX0111).

Data availability

Data underlying the results presented in this paper are not publicly available at this time but may be obtained from the authors upon reasonable request.

CRediT authorship contribution statement

Wubulitalifu Dawuti: Writing – original draft, Software, Resources, Methodology, Formal analysis, Data curation. **Jingrui Dou:** Resources. **Jintian Li:** Data curation. **Rui Zhang:** Validation. **Jing Zhou:** Resources. **Maierhaba Maimaitiaili:** Investigation. **Run Zhou:** Software. **Renyong Lin:** Conceptualization. **Guodong Lü:** Supervision, Conceptualization, Funding acquisition, Writing – review & editing.

Declaration of Competing Interests

Disclosures. The authors declare that there are no conflicts of interest related to this article.

References

[1] R.W. Krell, A.C. Wei, Gallbladder cancer: surgical management, Chin. Clin. Oncol. 8 (4) (2019) 36.
[2] M.A. Schmidt, L. Marcano-Bonilla, L.R. Roberts, Gallbladder cancer: epidemiology and genetic risk associations, Chin. Clin. Oncol. 8 (4) (2019) 31.
[3] H. Sung, J. Ferlay, R.L. Siegel, M. Laversanne, I. Soerjomataram, A. Jemal, F. Bray, Global cancer statistics 2020: GLOBOCAN estimates of incidence and mortality worldwide for 36 cancers in 185 countries, CA Cancer J. Clin. 71 (3) (2021) 209–249.
[4] S.K. Mishra, N. Kumari, N. Krishnani, Molecular pathogenesis of gallbladder cancer: an update, Mutat. Res. 816-818 (2019), 111674.
[5] M. Javle, H. Zhao, G.K. Abou-Alfa, Systemic therapy for gallbladder cancer, Chin. Clin. Oncol. 8 (4) (2019) 44.
[6] J. Ferlay, M. Colombet, I. Soerjomataram, C. Mathers, D.M. Parkin, M. Pineros, A. Znaor, F. Bray, Estimating the global cancer incidence and mortality in 2018: GLOBOCAN sources and methods, Int. J. Cancer 144 (8) (2019) 1941–1953.
[7] C.C. Wang, M.C. Tsai, S.C. Wang, C.M. Peng, H.L. Lee, H.Y. Chen, T.W. Yang, C. C. Lin, W.W. Sung, Favorable gallbladder cancer mortality-to-incidence ratios of countries with good ranking of world's health system and high expenditures on health, BMC Public Health 19 (1) (2019) 1025.
[8] A.A. Azizi, A. Lamarca, M.G. McNamara, J.W. Valle, Chemotherapy for advanced gallbladder cancer (GBC): a systematic review and meta-analysis, Crit. Rev. Oncol. Hematol. 163 (2021), 103328.
[9] L. Hickman, C. Contreras, Gallbladder cancer: diagnosis, surgical management, and adjuvant therapies, Surg. Clin. N. Am. 99 (2) (2019) 337–355.
[10] R. Kanthan, J.L. Senger, S. Ahmed, S.C. Kanthan, Gallbladder cancer in the 21st century, J. Oncol. 2015 (2015), 967472.
[11] T. Lin, Y.L. Song, J. Liao, F. Liu, T.T. Zeng, Applications of surface-enhanced Raman spectroscopy in detection fields, Nanomedicine (Lond) 15 (30) (2020) 2971–2989.
[12] M.A. Tahir, N.E. Dina, H. Cheng, V.K. Valev, L. Zhang, Correction: surface-enhanced Raman spectroscopy for bioanalysis and diagnosis, Nanoscale 13 (32) (2021) 13906.
[13] F. Lussier, V. Thibault, B. Charron, G.Q. Wallace, J.-.F. Masson, Deep learning and artificial intelligence methods for Raman and surface-enhanced Raman scattering, TrAC Trends Anal. Chem. 124 (2020), 115796.
[14] M.E. Ozer, P.O. Sarica, K.Y. Arga, New machine learning applications to accelerate personalized medicine in breast cancer: rise of the support vector machines, OMICS 24 (5) (2020) 241–246.
[15] N.M. Ralbovsky, I.K. Lednev, Towards development of a novel universal medical diagnostic method: Raman spectroscopy and machine learning, Chem. Soc. Rev. 49 (20) (2020) 7428–7453.
[16] L.W. Shang, D.Y. Ma, J.J. Fu, Y.F. Lu, Y. Zhao, X.Y. Xu, J.H. Yin, Fluorescence imaging and Raman spectroscopy applied for the accurate diagnosis of breast cancer with deep learning algorithms, Biomed. Opt. Express 11 (7) (2020) 3673–3683.
[17] J. Wang, D. Lin, J. Lin, Y. Yu, Z. Huang, Y. Chen, J. Lin, S. Feng, B. Li, N. Liu, R. Chen, Label-free detection of serum proteins using surface-enhanced Raman spectroscopy for colorectal cancer screening, J. Biomed. Opt. 19 (8) (2014), 087003.
[18] S.X. Li, Q.Y. Zeng, L.F. Li, Y.J. Zhang, M.M. Wan, Z.M. Liu, H.L. Xiong, Z.Y. Guo, S. H. Liu, Study of support vector machine and serum surface-enhanced Raman spectroscopy for noninvasive esophageal cancer detection, J. Biomed. Opt. 18 (2) (2013) 27008.
[19] Z.M. Zhang, S. Chen, Y.Z. Liang, Baseline correction using adaptive iteratively reweighted penalized least squares, Analyst 135 (5) (2010) 1138–1146.
[20] R. Gautam, S. Vanga, F. Ariese, S. Umapathy, Review of multidimensional data processing approaches for Raman and infrared spectroscopy, EPJ Tech. Instrum. 2 (1) (2015) 1.
[21] W. Dawuti, X. Zheng, H. Liu, H. Zhao, J. Dou, L. Sun, J. Chu, R. Lin, G. Lu, Urine surface-enhanced Raman spectroscopy combined with SVM algorithm for rapid diagnosis of liver cirrhosis and hepatocellular carcinoma, Photodiagnosis Photodyn. Ther. 38 (2022), 102811.
[22] C. Chen, F. Chen, B. Yang, K. Zhang, X. Lv, C. Chen, A novel diagnostic method: FT-IR, Raman and derivative spectroscopy fusion technology for the rapid diagnosis of renal cell carcinoma serum, Spectrochim. Acta A Mol. Biomol. Spectrosc. 269 (2022), 120684.
[23] V.E. Sitnikova, M.A. Kotkova, T.N. Nosenko, T.N. Kotkova, D.M. Martynova, M. V. Uspenskaya, Breast cancer detection by ATR-FTIR spectroscopy of blood serum and multivariate data-analysis, Talanta 214 (2020), 120857.
[24] M. Blanco-Formoso, R.A. Alvarez-Puebla, Cancer diagnosis through SERS and other related techniques, Int. J. Mol. Sci. 21 (6) (2020), 2253.
[25] Y. Zhang, X. Ye, G. Xu, X. Jin, M. Luan, J. Lou, L. Wang, C. Huang, J. Ye, Identification and distinction of non-small-cell lung cancer cells by intracellular SERS nanoprobes, RSC Adv. 6 (7) (2016) 5401–5407.
[26] K. Zhang, C. Hao, Y. Huo, B. Man, C. Zhang, C. Yang, M. Liu, C. Chen, Label-free diagnosis of lung cancer with tissue-slice surface-enhanced Raman spectroscopy and statistical analysis, Lasers Med. Sci. 34 (9) (2019) 1849–1855.
[27] M. Kashif, M.I. Majeed, M.A. Hanif, A.U. Rehman, Surface Enhanced Raman Spectroscopy of the serum samples for the diagnosis of Hepatitis C and prediction of the viral loads, Spectrochim. Acta A Mol. Biomol. Spectrosc. 242 (2020), 118729.
[28] H.F. Nargis, H. Nawaz, H.N. Bhatti, K. Jilani, M. Saleem, Comparison of surface enhanced Raman spectroscopy and Raman spectroscopy for the detection of breast cancer based on serum samples, Spectrochim. Acta A Mol. Biomol. Spectrosc. 246 (2021), 119034.
[29] K. Zhang, X. Liu, B. Man, C. Yang, C. Zhang, M. Liu, Y. Zhang, L. Liu, C. Chen, Label-free and stable serum analysis based on Ag-NPs/PSi surface-enhanced Raman scattering for noninvasive lung cancer detection, Biomed. Opt. Express 9 (9) (2018) 4345–4358.
[30] S. Li, Y. Zhang, J. Xu, L. Li, Q. Zeng, L. Lin, Z. Guo, Z. Liu, H. Xiong, S. Liu, Noninvasive prostate cancer screening based on serum surface-enhanced Raman spectroscopy and support vector machine, Appl. Phys. Lett. 105 (9) (2014) 91104.
[31] Y. Hong, Y. Li, L. Huang, W. He, S. Wang, C. Wang, G. Zhou, Y. Chen, X. Zhou, Y. Huang, W. Huang, T. Gong, Z. Zhou, Label-free diagnosis for colorectal cancer through coffee ring-assisted surface-enhanced Raman spectroscopy on blood serum, J. Biophotonics 13 (4) (2020), e201960176.
[32] J.L. Gonzalez-Solis, J.C. Martinez-Espinosa, L.A. Torres-Gonzalez, A. Aguilar-Lemarroy, L.F. Jave-Suarez, P. Palomares-Anda, Cervical cancer detection based on serum sample Raman spectroscopy, Lasers Med. Sci. 29 (3) (2014) 979–985.
[33] S. Feng, R. Chen, J. Lin, J. Pan, G. Chen, Y. Li, M. Cheng, Z. Huang, J. Chen, H. Zeng, Nasopharyngeal cancer detection based on blood plasma surface-enhanced Raman spectroscopy and multivariate analysis, Biosens. Bioelectron. 25 (11) (2010) 2414–2419.
[34] C. Chen, G. Du, D. Tong, G. Lv, X. Lv, R. Si, J. Tang, H. Li, H. Ma, J. Mo, Exploration research on the fusion of multimodal spectrum technology to improve performance of rapid diagnosis scheme for thyroid dysfunction, J. Biophotonics 13 (2) (2020), e201900099.
[35] T.D. Vu, E. Jang, J. Lee, D. Choi, J. Chang, H. Chung, Feasibility of voltage-applied SERS measurement of bile juice as an effective analytical scheme to enhance discrimination between gall bladder (GB) polyp and GB cancer, Anal. Chem. 92 (12) (2020) 8159–8169.
[36] K.V. Serebrennikova, A.N. Berlina, D.V. Sotnikov, A.V. Zherdev, B.B. Dzantiev, Raman scattering-based biosensing: new prospects and opportunities, Biosensors (Basel) 11 (12) (2021) 512.